Astronomy & Astrophysics manuscript no. thorium˙paper˙modif
December 30, 2011

The Hamburg/ESO R-process Enhanced Star survey (HERES) ⋆

VII. Thorium abundances in metal-poor stars

J. Ren[1,2,3], N. Christlieb[2], and G. Zhao[1,4]

[1] The School of Space Science and Physics, Shandong University at Weihai, Wenhua Xilu 180, 264209 Weihai, Shandong, China
e-mail: renjing@bao.ac.cn,gzhao@nao.cas.cn
[2] Zentrum für Astronomy der Universität Heidelberg, Landessternwarte, Königstuhl 12, D-69117 Heidelberg, Germany
e-mail: N.Christlieb@lsw.uni-heidelberg.de
[3] Department of Physics and Astronomy, Uppsala University, Box 516, 751 20 Uppsala, Sweden
[4] Key Laboratory of Optical Astronomy, National Astronomical Observatories, CAS, 20A Datun Road, 100012 Chaoyang District, Beijing, China

Received / Accepted

ABSTRACT

We report thorium abundances for 77 metal-poor stars in the metallicity range of $-3.5 < [\mathrm{Fe/H}] < -1.0$, based on "snapshot" spectra obtained with VLT-UT2/UVES during the HERES Survey. We were able to determine the thorium abundances with better than 1σ confidence for 17 stars, while for 60 stars we derived upper limits. For five stars common with previous studies, our results were in good agreement with the literature results. The thorium abundances span a wide range of about 4.0 dex, and scatter exists in the distribution of log(Th/Eu) ratios for lower metallicity stars, supporting previous studies suggesting the r-process is not universal. We derived ages from the log(Th/Eu) ratios for 12 stars, resulting in large scattered ages, and two stars with significant enhancement of Th relative to Eu are found, indicating the "actinide boost" does not seem to be a rare phenomenon and thus highlighting the risk in using log(Th/Eu) to derive stellar ages.

Key words. Stars: abundances – Stars: population II – Galaxy: abundances – Galaxy: evolution – Galaxy: halo

1. Introduction

The observed chemical abundances of metal-poor stars provide rich information on star formation and nucleosynthesis in the early stages of evolution of our galaxy and other galaxies. In particular, the study of heavy elements beyond the iron group in metal-poor stars have greatly improved the understanding of the neutron-capture nucleosynthesis processes in the early Universe, e.g., placing constraints on the astrophysical site(s) of r-process. Neutron-capture elements in r-process enhanced metal-poor stars have been reported to match the scaled solar r-process abundance pattern at least in the range of $\mathrm{Z} = 52 \sim 76$ (see e.g., Cowan et al. 2002; Sneden et al. 2003; Honda et al. 2004). In contrast, lighter elements ($\mathrm{Z} < 50$) abundances deviate significantly from the Solar-pattern, indicating the existence of different initial production ratios for the r-process elements (Sneden et al. 2000, 2003; Honda et al. 2004). In old, metal-poor stars, thorium and uranium with relatively long half-life are the only heavier r-process elements we could observe today, and offer a way to better understand the heaviest products in r-process nucleosynthesis (Roederer et al. 2009).

The detection of the radioactive-decay elements in r-process enhanced metal-poor stars allowed a new approach to derive the age of the oldest stars, by means of comparing the observed ratios of radioactive decay elements over stable elements with the corresponding initial values at the time when the star was born[1], hence providing a lower limit on the age of the universe. The actinide thorium is one such radioactive species. It is produced in the r-process, and has been widely used, particularly log(Th/Eu), for cosmochronometry to estimate stellar ages (e.g., Sneden et al. 1996; Hill et al. 2002; Honda et al. 2004; Frebel et al. 2007; Hayek et al. 2009). Some authors have argued that log(Th/Eu) is not a reliable chronometer to derive stellar ages, because of the relatively large uncertainties (e.g., Goriely & Clerbaux 1999; Goriely & Arnould 2001; Honda et al. 2004; Frebel et al. 2007). Due to its longer half-life of 14.05 Gyr as compared with, say, 4.5 Gyr of uranium, some authors have suggested that the log(U/Th) pair would be a better chronometer, because of their close atomic number and thus relatively small nuclear physics uncertainties (Cayrel et al. 2001; Wanajo et al. 2002; Beers & Christlieb 2005). Additionally, because Pb and Bi mostly originate from α-decay of the Th and U isotopes, the measurement of Pb or Bi abundances can offer a consistency check on the calculated initial abundances for this pair (Cowan et al. 1999). However, it is very difficult to detect U lines in stellar spectra, due to the blending of the weak U lines (e.g., 3859 Å) and the relatively low amount of uranium in an old star with age of $\sim 12 - 15$ Gyr (see Plez et al. 2004; Roederer et al. 2009). Alternatively, Hf behaves similarly to third-peak elements and the log(Th/Hf) ratio has been suggested by Kratz et al. (2007) as a promising tool for chronometer studies.

⋆ Based on observations collected at the European Southern Observatory, Paranal, Chile (Proposal Number 68.B-0320).

[1] Accurately speaking, it was the time when the radioactive decay elements were produced, not necessarily to be the same as when the star was born.

Many efforts have been made to determine thorium abundances in metal-poor stars using high resolution spectra. So far, more than 30 metal-poor stars ($[\mathrm{Fe/H}] < -1$) have been reported with thorium abundances in previous studies, and the error is typically of order of 0.15 dex. It appears that among the r-process enhanced stars with measured Th or other actinide elements (e.g.,U), except for an actinide normal group, which means no obvious enhancement of actinide element abundances with respect to the scaled solar r-process pattern, an actinide boost group (e.g., CS31082-001, HE1219-0312, CS30306-132) also came to be known, although the former group seems to be more common among r-process enhanced metal-poor stars (e.g., CS22892-052, CS29497-004). This imples that for elements in the range of Z $\geq$ 90, significantly different chemical yields might be produced due to the various conditions of the star formation regions (Hill et al. 2002; Roederer et al. 2009; Mashonkina et al. 2010).

To obtain accurate age estimates and to explore r-process nucleosynthesis in metal-poor stars in detail, high-precision Th abundances are needed. Further, large samples of stars with Th abundances are also important to study the distribution of thorium abundances in metal-poor stars. The HERES survey offers a good opportunity to perform such a study. More than 22 elemental abundances (not including Th) for the sample stars have been reported in previously published papers in this series(e.g., Barklem et al. 2005; Zhang et al. 2010), and thorium abundances have been studied furtherly with better quality spectra in a few stars (Hayek et al. 2009; Mashonkina et al. 2010).

Here we report thorium abundances for 77 stars from the sample of Barklem et al. (2005) (hereafter Paper II), using a modified version of the analysis method described in that paper. A brief description of the sample is given in sect. 2. The abundance analysis is described in sect. 3. In sect. 4, thorium abundances are presented and compared with previous works, and the implications for stellar age estimates are discussed. Section 5 presents the conclusions.

2. The sample

This work is based on the moderately high-resolution "snapshot" spectra of 253 HERES stars. Readers are referred to Christlieb et al. (2004) and Paper II for detailed information on the observations and the sample selection. For convenience, we repeat the most important basic information on the sample. The spectra ($R \sim 20000$, $\lambda = 3760 - 4980$ Å , and typical $S/N \sim 30$ to 50) were obtained during the HERES survey with ESO-VLT2/UVES. A total of 373 spectra were observed, which was reduced to 253 stars in Paper II when stars were removed for various reasons, most importantly due to strong molecular carbon features leading to significant blending. Much of the remainder of the sample has been analysed by Lucatello et al. (2006). These 253 stars are the starting point for our analysis; however, reasonable estimates of Th abundances or even upper limits could not be obtained for all stars for reasons that will be discussed further below.

3. Abundance analysis

We derive abundances from the Th II 4019.12 Å line, the only Th line strong enough to be detected in our spectra. This line is unfortunately blended, including blends of ^{13}CH. The line has been analysed using the automated spectrum analysis code based on SME (Valenti & Piskunov 1996) described in Paper II and used in Jonsell et al. (2006) (hereafter Paper III). The stellar parameters and abundances of other elements, particularly those giving rise to blends with the Th line, were adopted directly from Paper II. In order to be able to model the ^{13}CH blends, some modifications were made to the code to enable estimates of the ^{12}C/ ^{13}C ratio to be obtained. This ratio has been determined from isolated ^{13}CH features between 4210 and 4225 Å and at 4370 Å, as shown in Paper III, though now in an automated manner.

Table 1. Line list.

Species	λ [Å]	ξ [eV]	$\log gf$	Refs.
Th II	4019.129	0.000	−0.228	1
^{13}CH I	4019.000	0.460	−1.163	2
^{13}CH I	4019.170	0.460	−1.137	2
Fe I	4019.050	2.608	−2.780	3
Co I	4019.110	2.280	−3.287	2
Co I	4019.118	2.280	−3.173	
Co I	4019.120	2.280	−3.876	
Co I	4019.125	2.280	−3.298	
Co I	4019.125	2.280	−3.492	
Co I	4019.134	2.280	−3.287	
Co I	4019.135	2.280	−3.474	
Co I	4019.138	2.280	−3.173	
Co I	4019.140	2.280	−3.298	
Co I	4019.272	0.580	−3.480	2
Co I	4019.281	0.580	−3.470	
Co I	4019.294	0.580	−3.220	
Co I	4019.296	0.580	−3.330	
Co I	4019.322	0.580	−4.090	
Co I	4019.332	0.580	−4.040	
Ni I	4019.058	1.935	−3.174	2
Ce II	4019.057	1.014	0.093	2
Nd II	4018.836	0.060	−0.880	2

References. (1) - Nilsson et al. (2002), (2) - Johnson & Bolte (2001) (3) - Kupka et al. (1999)

The employed line data is shown in Table 1, and is essentially that of Johnson & Bolte (2001). The f value for the Th II line has been updated (a change of +0.05 dex) and the wavelengths and excitation potentials have been negligibly changed in some cases based on VALD values (Kupka et al. 1999). All blends within 0.5 Å either side of the Th line in the list of Johnson & Bolte (2001) are included, except a line of U and and a line of V, which we are unable to model since we do not have abundances for these elements; their contributions are expected to be negligible in any case. A window 0.3 Å wide centred on the Th line is used for the fitting.

In Paper II we required at least one line to be detected at the 3σ confidence level to claim an elemental detection. Such a high threshold would result in a very small number of detections given the weakness of the single Th line we used and the quality of our spectra. Here we reduce this requirement to 1σ, though with some additional constraints. First, the significance of detection was caculated from the fit without blending, i.e., $m' = m \times (1 - d_{\rm b}/d_{\rm fit})$, where $d_{\rm b}$ and $d_{\rm fit}$ are the line depths of the blendings (without thorium line) and the whole fit respec-

tively; m is the detection level of the the whole fit. Second, all lines calculated to have m above the 1σ detection level were subjected to manual inspection and adjustment adopted for some stars, usually due to noise or severe blending casting significant doubt on its validity. Finally, except for several stars raised to detection level considering their strong line strengths, for all other stars with detections m' below the 1σ confidence level and those rejected during manual inspection, we calculated 1σ upper limits, but rejecting those with uncertain upper limits, i.e., blendings occupying more than 80% of the fit or one of the fits not converged.

The errors in the abundances could in principle be estimated using the methods of Paper II, but is complicated by the additional uncertainties from blending. In Paper II we found relative and absolute errors of ~ 0.18 and ~ 0.25 dex, respectively, for species with similar atomic structure to Th II, and thus lines with similar sensitivities to stellar parameters, e.g. Nd II, Sm II, Eu II. These cases have more and stronger lines and no significant blending issues. Accounting for these extra sources of error we estimate relative and absolute errors in the Th abundances of ~ 0.25 and ~ 0.3 dex, respectively. Similarly, by comparison with errors in Nd/Eu etc., an error of ~ 0.25 dex is estimated for the abundance ratio log(Th/Eu).

However, it should be noted that, in our analysis, we have adopted the detection significance of 1σ, which means the statistic uncertainty will dominate the general error. Thus, we value any interesting results from our analysis, but are very cautious to give any conclusion based on our results.

4. Results

The detected thorium abundances for stars classified into different subclasses are tabulated in Table 4. In Table 5 (online only), stars with upper limits are included, together with the atmospheric parameters and some other abundances of interest from Paper II. The confidence level of the detection $m\sigma$ and $m'\sigma$, computed as described in section 3.4 of Paper II and in section 3 of this paper, are also tabulated. The errors are not listed since they are either the same for all stars in the cases involving Th (see above), or available in Paper II.

Throughout this discussion we classify different types of neutron-capture stars according to Beers & Christlieb (2005) as summarized in Table 3. In addition, we adopt the definition of s-II stars from Paper II. Compared with the s subclass, s-II stars actually are those with both strong r- and s- process enhancement ($[\mathrm{Ba/Fe}] > 1.5$, $[\mathrm{Eu/Fe}] > 1.0$ and $[\mathrm{Ba/Eu}] > 0.5$).

We note, HE1221-1948 is one of the several C-enhanced stars ([C/Fe]=1.42) in our analysis, which has been analysed by Lucatello et al. (2006) manually, giving a metallicity of -2.60 and [Eu/Fe]=2.1. Since in Paper II, it was mentioned that our method is not suitable for C-rich stars spectra, and actually this star was noticed in figure 5 of Paper II with $\Delta[\mathrm{Fe/H}] > 1$ comparing the final [Fe/H] with the initial estimate, thus in this work we demote this star to an upper limit, although $m' > 1$ was obtained, which we subjected to an overestimated $\mathrm{S/N}$. HE1221-1948 is the only carbon rich one ($[\mathrm{C/Fe}] > 1$) among the most metal-poor stars ($[\mathrm{Fe/H}] < -3.0$) with detected thorium abundances in our sample.

4.1. Thorium abundances distribution

In the sample of 253 stars, finally we obtain thorium abundances[2] for 17 stars. For another 60 stars, we obtained upper limits. In Fig. 1, we give the thorium abundances distribution of these stars. We were unable to derive the thorium abundance for the other 176 stars, 79 of which were set aside for various reasons, the most common being that the spectrum was too contaminated with blends to derive anything reliable given the resolution of the observed spectrum. We adopted 1σ detection level, and since our aim is to investigate the general trend of thorium abundances, this detection level is adequate to give a reliable distribution.

As shown in Fig.1, in the distribution of thorium abundances by the 1σ detection, majority of the stars lie in the range of -2.0 to -1.0, about 82% of all the detections, and the distribution including 1σ upper limits extends from -3.0 to 1.0, having a peak at -2.0 to -1.0. The thorium abundance results in previous studies all fall in this range (see e.g., Roederer et al. 2009; Honda et al. 2004). In the lower panel of Fig.1, the only one detection above 3σ is owned by CS31082-001, which has $\log\epsilon(\mathrm{Th}) = -1.00$, and including those with 3σ upper limits the distribution spaning from -3.0 to 1.5, has a peak at the range of -1.0 to -0.5. Only the higher Th abundances side of this histogram can give useful information about the true shape of the cosmic distriubtion, since there is a natural detection bias towards larger abundances. The existence of a large scatter in thorium abundances among metal-poor stars as seen from this histogram can be explained by the poor mixing in the early universe.

However, because the abundance of thorium is based on one single Th II line $4019\,\text{Å}$, it should be borne in mind the that Th abundance is susceptible to errors due the difficulties in modelling the blends. The line Th II $4019\,\text{Å}$ is blended with temperature sensitive spectral features, such as Co and Ni, thus, we expect some degree of the scatter is due to errors in the analysis, e.g., uncertain Teff, rather than real cosmic scatter. However, as shown in Fig.1 and Fig. 3 of this paper, the scatter significantly exceeds the estimated errors, and thus given the detection bias, it gives a lower limit to the range of the true cosmic distribution.

4.2. Comparation with previous studies

As shown in Table 2, we obtained Th abundances for five stars which have been studied previously in detail with similar or better quality observational data by others, namely CS 22892−052, CS 29497−004, CS 31082−001, CS 29491−069 and HE 2327−5642. Note that we failed to derive the thorium abundance for a well studied bright halo star HE 221170, since our modelling indicated Th II line in this star to be severely blended by Co lines; this star has been reported thorium enhanced compared with iron (Ivans et al. 2006; Yushchenko et al. 2005). The same for another strongly r-process enhanced star HE 1219−0312, in which the blendings exceed 80% of the line fit, resulting a very uncertain abundance. HE 0338−3945 is an reported s-II carbon enhanced star ([Eu/Fe = 1.89, [Ba/Eu] = 0.52, and [C/Fe] = 2.07]), which experienced strongly both r- and s- process enhancements. For the same reason as for other carbon-enhanced stars, our method failed to get a reliable thorium abundance for this hot dwarf. For rest of the

[2] Here we adopt the standard spectroscopic notations:
$\log\epsilon(\mathrm{A}) = \log_{10}(N_\mathrm{A}/N_\mathrm{H}) + 12$ for abundances;
$[\mathrm{A/B}] = \log_{10}(N_\mathrm{A}/N_\mathrm{B})_\star - \log_{10}(N_\mathrm{A}/N_\mathrm{B})_\odot$ for relative abundances;
log(A/B)=logϵ(A)-logϵ(B) for abundance ratios.

Table 2. Comparison with literature results for seven common stars

	$T_{\rm eff}$ [K]	log$g$ [cm s^{-2}]	[Fe/H]	$V_{\rm mic}$ [km s^{-1}]	logϵ(Th)	Notes
CS 22892−052	4884	1.81	−2.95	1.67	−1.76	This work
	4790	1.6	−2.92	1.8	-1.42 ± 0.15	Honda et al. (2004)
	4800	1.5	−3.1	1.95	-1.57 ± 0.10	Sneden et al. (2003)
	4710	1.5	−3.2	2.1	-1.60 ± 0.07	Sneden et al. (2000)
	4800	1.5	−3.1	1.95	-1.60 ± 0.13	Roederer et al. (2009)
CS 29497−004	5013	2.23	−2.81	1.62	−1.17	This work
	5090	2.4	−2.81	1.6	-0.96 ± 0.15	Christlieb et al. (2004)
CS 31082−001	4922	1.90	−2.78	1.88	−1.00	This work
	4825	1.5	−2.9	1.8	-0.98 ± 0.05	Hill et al. (2002)
			−2.9		-0.98 ± 0.05	Plez et al. (2004)
	4790	1.8	−2.81	1.9	-0.92 ± 0.10	Honda et al. (2004)
CS 29491−069	5103	2.45	−2.81	1.54	< -1.37	This work
	5300	2.8	−2.6	1.6	-1.46 ± 0.25	Roederer et al. (2009)
	5300	2.8	−2.6	1.6	-1.43 ± 0.22	Hayek et al. (2009)
HE 2327−5642	5048	2.22	−2.95	1.69	−1.45	This work
	5050	2.34	−2.78	1.8	-1.67 ± 0.20	Mashonkina et al. (2010)

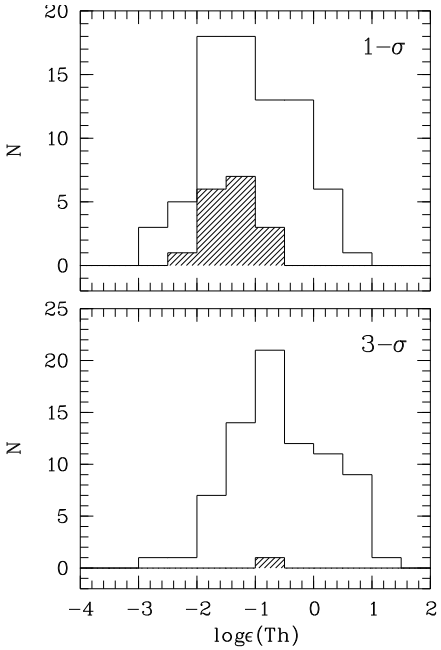

Fig. 1. Histogram of derived thorium abundances. 1σ (upper panel) and 3σ (lower panel) detections are displayed. The shadow plots show the stars with detected abundances, while the blanks also include stars with upper limits.

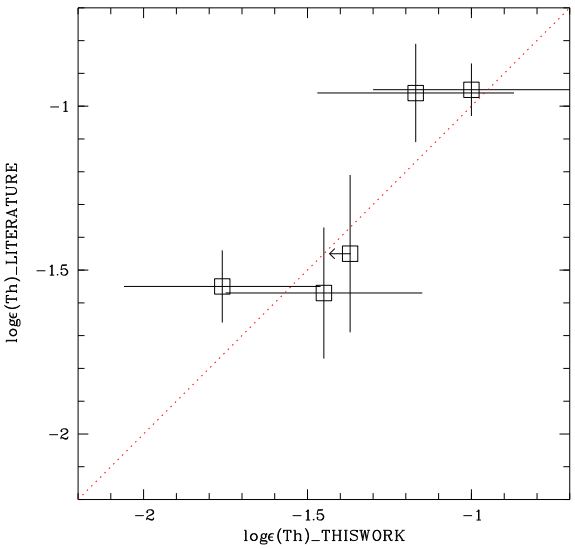

Fig. 2. Thorium abundances comparison for the common stars between this work and previous works, which are the averaged value if there are more than one results. Error bars are given and upper limits are marked with arrows.

common stars, our thorium abundance results are all in agreement with literatures values within the uncertainty as shown in Fig. 2; such consistence gives us the confidence that our results are reliable for studying the overall thorium abundances distribution of metal-poor stars.

In Fig. 3, we plot thorium abundances and the ratios of thorium over europium against increasing metallicity, and we also plot results collected from previous studies in green, including field halo stars (e.g., Cayrel et al. 2001; Hill et al. 2002; Frebel et al. 2007; Roederer et al. 2009), globular clusters M5 and M15 (Yong et al. 2008a,b), and a member of a nearby dwarf spheroidal galaxy (Aoki et al. 2007). Filled symbols are used to mark the common stars listed in 2, while due to different metallicities adopted, they look not in pairs. In the lower panel a "zero-age" line caculated based on the initial ratio $\log\epsilon({\rm Th/Eu})_0 = -0.33$ given by Schatz et al. (2002) is shown, and we will discuss more about age estimations in section 4.4. Stars with both detected and upper limits of thorium abundances at the $\geq 1\sigma$ level are included. Europium and other element abundances in this work are from the analysis of Paper II. A summary of previous results on thorium abundances is given in online Table 6.

In the upper panel of Fig. 3, we see our sample provides detections which extend the range of derived thorium abundances to lower metallicities. At [Fe/H] < -1.8, a larger scatter can be seen, as expected according to the scenario of poor mixing in the very early universe. No clear trend with increasing metallicity is seen, but the averaged detected logϵ(Th) is ~ 0.4 dex lower than those with metallicity above -1.8. Due to lack of derived Eu abundances, stars at the low metallicity end, e.g., HE 0353−6024 with the lowest metallicity of -3.17 in the

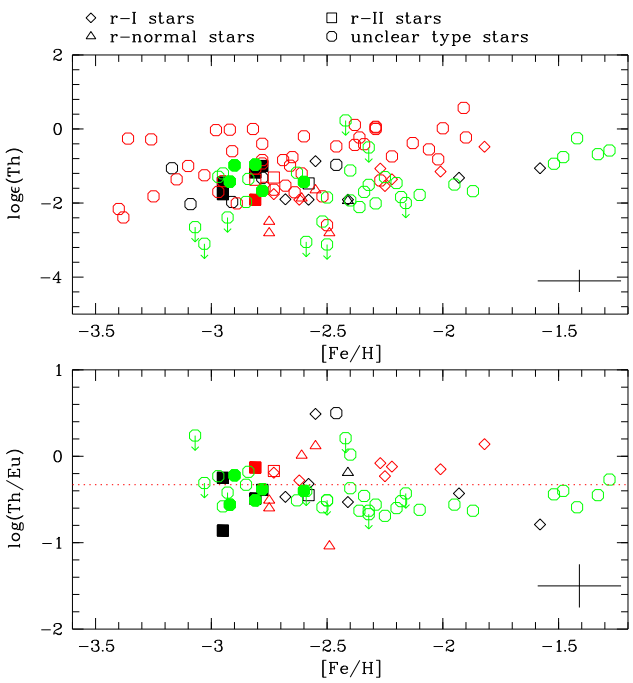

Fig. 3. Plot of logϵ(Th) vs. [Fe/H] and log(Th/Eu) vs. [Fe/H]. Detected results from this work are in black, and the upper limits are in red. Results from other studies are in green. These filled symbols are the stars in common with previous works. See text for the definations of different subclasses. A dashed red line is plotted in the lower panel corresponding to the "zero-age" log(Th/Eu). Averaged error bars are given at the lower right corner.

Table 3. Definition of subclasses of metal-poor stars

Class	Constraints
r-normal	$0 \leq [\mathrm{Eu/Fe}] < 0.3$ and $[\mathrm{Ba/Eu}] < 0$
r-I	$0.3 \leq [\mathrm{Eu/Fe}] \leq 1.0$ and $[\mathrm{Ba/Eu}] < 0$
r-II	$[\mathrm{Eu/Fe}] > 1.0$ and $[\mathrm{Ba/Eu}] < 0$
s	$[\mathrm{Ba/Fe}] > 1.0$ and $[\mathrm{Ba/Eu}] > 0.5$
s-II	$[\mathrm{Eu/Fe}] > 1.0$ and $[\mathrm{Ba/Eu}] > 0.5$
r/s	$0.0 < [\mathrm{Ba/Eu}] < 0.5$

upper panel were lost in the lower panel. The distribution of log(Th/Eu) ratios spans from -0.86 to 0.50, while considering the uncertainty, most of them are consistently close to the "zero-age" line, supporting the universal r-process pattern in the early universe, except for only two stars: r-I star HE 0105−6141 and HE 1332−0309 with no clear type yet, which have much higher logϵ(Th/Eu) of 0.49 dex and 0.50 dex, respectively. They might belong to the so-called "actinide boost" star group, which we will discuss again in section 4.4.

4.3. Correlation with other neutron capture elements

Correlations between abundances of thorium and other neutron-capture elements are used to explore the nature of nucleosynthesis, and impose contraints on astrophysical and nuclear models. Chemical abundance analysis suggest that for elements with $Z = 52 \sim 76$, the abundance pattern is consistent with the scaled solar system r-process abundance distribution. Recent studies have found relatively low abundance levels for light elements ($Z < 50$) compared with heavy elements, which suggest two distinct types of r-process events, a main r-process for the elements above the second-peak elements, and a weak r-process for lighter neutron capture elements. The enhancement of actinides with respect to the rare earth elements were also noticed in some stars.

In this work, we also explored the correlations between thorium and other neutron-capture elements. In Fig. 4, we plot the ratios of Th abundances against Ba, Sr and Y. There are larger scatters among the results of Th correlated with Ba and Sr, and usually the scatter comes from the unclear type stars, which indicates the existence of multiple nucleosynthesis prcesses. Scatter of [Ba/Fe] and [Sr/Fe] were also reported by other studies (McWilliam 1998; Norris et al. 2001). All these elements follow similar abundance pattern as thorium as expected, and stars of the same enhancement type have quite consistent distribution, supporting that they might form from the materials experienced similar chemical enrichments. Elemental ratios of log(Th/Ba), log(Th/Sr) and log(Th/Y) for almost all the stars are enhanced compared with the ratios in solar system. Two stars: HE 2219−0713 and HE 0353−6024 are particular interesting. The former star has more Th than Ba, and the latter one has more Th than Sr. As shown in Fig. 7, the Th II line is quite weak in both of the two stars, and even we can see some comparable "noise" or "features" unfitted, but since we failed to find the possible missing lines here, and our line list is believed to be well established, thus we suspect the S/N is overestimated for them, consequently leading to an overestimation of the detection significance. Better quality data for the two stars are needed to confirm this results.

In Fig. 5, the three chronometer ratios log(Th/Eu), log(Th/La) and log(Th/Nd) were plotted. Except the two stars with high enhancement of log(Th/Eu), all the other stars have consistent distribution with literature results, and the smaller scatter in the distributions, indicate the three age indicator will give consistent age estimations.

4.4. Implications for age estimations and nuclear astrophysics

The errors in Th abundance as well as the large scatter in the derived log(Th/Eu) ratios for metal-poor stars lead to significant uncertainties in age estimates. A 0.2 dex error in log(Th/Eu) will induce an error of 9.3 Gyr in age, which could be even more if considering the uncertainty in the predicted initial production ratios (PRs) (Frebel et al. 2007). In our case, the error of log(Th/Eu) is estimated to be > 0.25, which corresponds to an error of at least > 11.7 Gyr in age determinations. In addition, it is known that, due to the so-called "actinide boost" phenomenon, the log(Th/Eu) chronometer pair fails to give meaningful estimates of age for some objects, e.g., CS 30306−132, CS 31078−018, CS 31082−001 and HE 1219−0312, all giving negative ages. These objects exhibit higher abundances of thorium and uranium with respect to the lanthanides, which is currently not understood. Roederer et al. (2009) examined the Pb and Th abundances in 27 r-process only stars, and suggest that, deviation from main r-process affect at most only the elements beyong the third r-process peak elements, i.e., Pb, Th and

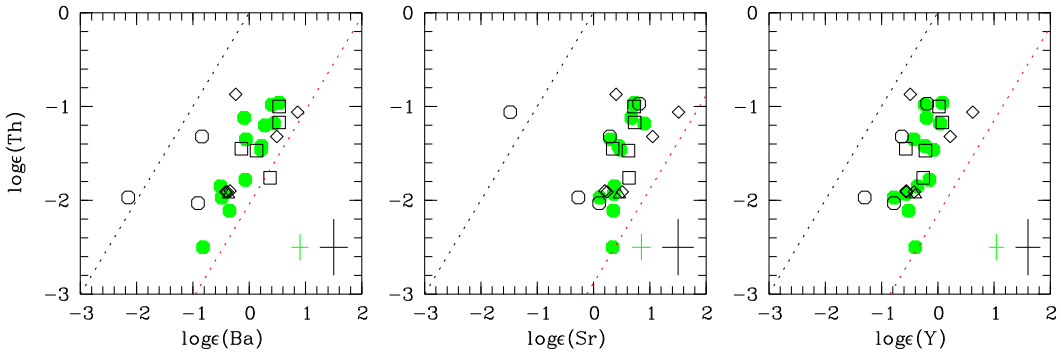

Fig. 4. logϵ(Th) plotted against neutron capture elements: Ba, Sr and Y. A diagonal 1:1 relation (black), and the solar ratio (red) are plotted for comparision. Error bars of the results from this work and the literature are given in the lower right of each plot. The symbols are as same as in Fig. 3. HE 2219−0713 has higher Th than Ba, and HE 0353−6024 has higher Th than Sr.

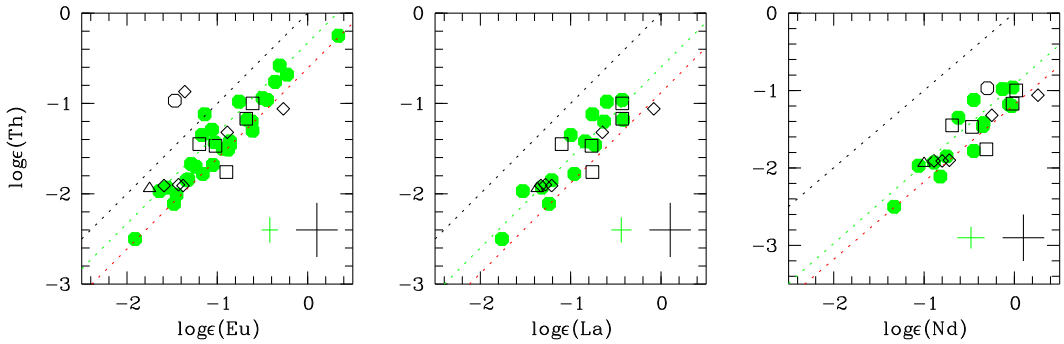

Fig. 5. logϵ(Th) plotted against neutron capture elements: Eu, La and Nd. A diagonal 1:1 relation (black), the initial ratio (green)(Schatz et al. 2002) and the expected ratio assuming an age of 13 Gyr (red) are plotted for comparision. Error bars are also given in the lower right of each plot. The symbols are as same as in Fig. 3. The two stars that have much higher Th than Eu are HE 0105−6141 and HE 1332−0309.

U, while the reason for the low amount of Pb in CS 31082−001 is not clear yet. Pb isotops and actinide elements measurements for more metal-poor stars are necessary for better understanding the nucleosynthesis in such actinide enhanced stars, and to explore how common this "actinide boost" phenomenon may exist in metal-poor stars.

Despite the large uncertainty in using log(Th/Eu) chronometer, it is meaningful to give the distribution of age estimations for so far the largest old population sample with avaliable log(Th/Eu). In Fig. 6, against [Fe/H], derived ages and the deviations of our expected initial production ratios (PRs), from the present theoretic initial PRs are plotted. We caculated the expected PRs assuming an age of 13 Gyr for all the stars, since these stars are expected to be very old based on their low metallicities. For age estimation we adopted $\log(\mathrm{PR}) = -0.33$ from Schatz et al. (2002), which is in the middle of other PRs (Sneden et al. 2003; Cowan et al. 2002; Frebel et al. 2007). Different PRs would only change the absolute age determinations by smalle amounts, i.e., ∼2-4 Gyr (Frebel et al. 2007). Stars (green) from previous studies are also included for comparison. Ages from log(Th/Eu), together with that from log(Th/La) and log(Th/Nd), if available, based on the initial PRs of Schatz et al. (2002), are plotted in black, red and blue respectively in the middle panel. Lines corresponding to different ages or in the lower panel, the zero-deviation lines corresponding to different age chronometers are plotted.

It can be seen from the plot that, the ages derived from log(Th/Eu) for those metal-poor stars in our sample are in general consistent with literature values within the uncertainty, except for HE 0105−6141 and HE 1332−0309, and there is no apparent trend with increasing metallicity. It's seen that the derived ages distribute around 13 Gyr and scatter below 0 Gyr, with several "negative age" stars as previously reported from other works, and also in this work. In upper panel of Fig. 3, HE 0105−6141 and HE 1332−0309 are in the higher end of continuous logϵ(Th) distribution, but the ratio of log(Th/Eu)

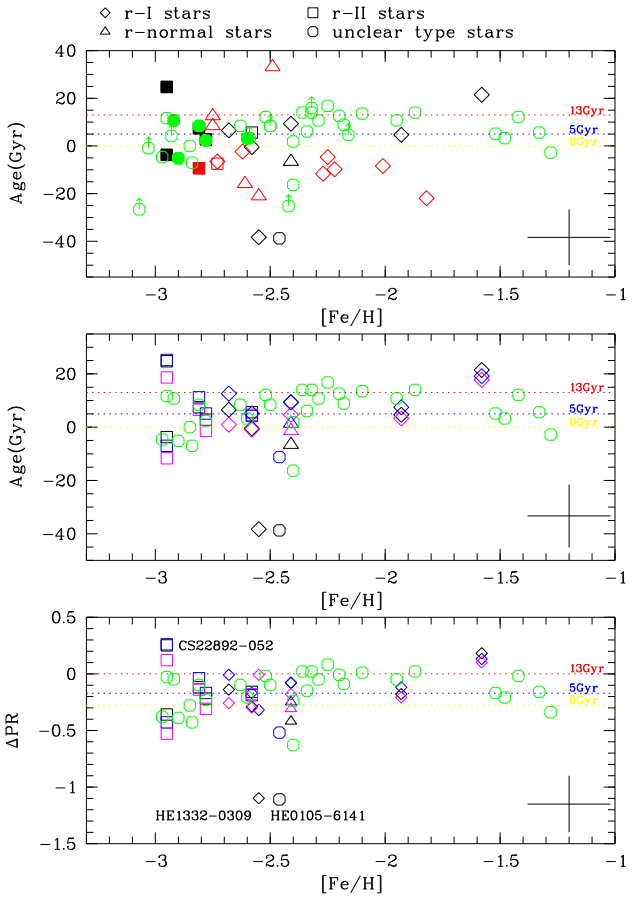

Fig. 6. Upper Panel: plot of ages derived from log(Th/Eu) against [Fe/H]; **Middle Panel:** ages derived from different chronometers; **Lower Panel:** plot of the differences between our expected initial production ratios and the theoretic predictions $\log(\mathrm{Th/Eu})_0$ against [Fe/H] assuming age of 13Gyr for all the stars. Symbols and colours are as same as in Fig. 3, and in the middle panel, we use black, red and blue symbols for results derived from log(Th/Eu), log(Th/La) and log(Th/Nd) respectively.

reach as high as ~ 0.5 dex, ~ 0.5 dex higher than other stars. Thus, if considering the limitations of our data set, only these two stars are very likely to be "actinide boosted".

In Fig. 7, the Th II line profile fits for stars above 1σ detection are displayed. The observed spectra are in solid black lines, and the noise on the spectra were overplotted in dotted black lines. A range of 3 Å fit region is highlighted in bright yellow. The red solid lines are the best fit synthetic profile and the red dotted lines are the profile fits with only blendings, from which it's easily seen how severe the Th II lines are blended. Star name, parameters, detection confidence m and m', and S/N are shown in the top of each plot. HE 1332−0309 has a low S/N of 31, and the observed line profile could't be reproduced well with present line list, which may due to low S/N or unresolved blendings in the Th II line region. HE 0105−6141 with higher S/N of 55, however also suffers from noise. We notice the blendings around Th II for the two stars are very light, which may also indicate that, some missing blending components might lead to an overestimation of Th abundance. Thus, better understanding of the blendings and higher quality data of these objects need to be obtained in the future to verify this preliminary result.

For the common star CS 31082−001, we derived $\log(\mathrm{Th/Eu}) = -0.39$, $\log(\mathrm{Th/La}) = -0.57$, $\log(\mathrm{Th/Nd}) = -1.02$, which is consistent with -0.22, -0.60, and -0.91 from Schatz et al. (2002) within the uncertainty. Although we got a very consistent Th abundance with Hill et al. (2002), we adopted a 0.15 dex higher Eu abundance from Paper II, which leads the offset in log(Th/Eu). We adopted the zero-age $\log(\mathrm{Th/X})_0$ (X is the stable r-process elements) ratios from Schatz et al. (2002), where they used solar abundances $\mathrm{X}_\odot$ instead of the r-process model predictions X_0, therefore, the discrepancies in the estimated ages from different log(Th/X) reflect deviations of the observed stellar abundances from a solar abundance pattern. As shown in the middle panel of Fig. 6, the deviations are tiny and similar for most stars, for which two or three chronometers are available, and log(Th/La) always gives the youngest ages, indicating compared with Eu and Nd, observed La abundances always have larger deviations from solar La abundance. For HE 0105−6141, only log(Th/Eu) and log(Th/Nd) are avaliable, the latter one gives a much older age, which may suggest the high log(Th/Eu) in this stars is due to an abnormal low Eu abundance, while so far no other studies give Eu abundance for this star.

From the bottom panel of Fig. 6, it shows if assuming a consistent age of 13 Gyr for these metal-poor stars, their intial production ratios for most of the stars seems needed to be increased by a factor up to 4, and even more if the two "actinide boost" stars are confirmed.

In order to explore more about these two unique stars, in Fig. 8, we plot their abundance patterns, compared with solar r- and s-process patterns scaled to Eu and Ba (or Sr) respectively. For HE 1332−0309, because no Ba abundance has been obtained, we scaled the solar s-process pattern to Sr. As comparison, a thorium normal r-II star CS22892−052, a previous reported "actinide boost" r-II star CS 31082−001 are also plotted. It can be seen from the plot, except for Th, the avaliable neutron-capture abundances of CS22892−052 follow the Solar pattern quite well, and the same is for CS 31082−001, but for both stars, we underestimated their log(Th/Eu) ratios. The situation is different for HE 0105−6141, for which the Th abundance was highly enhanced, but the other avaliable neutron-capture elements follow the Solar r-process pattern. For HE 1332−0309, Barium abundance is not avaliable. Beside Th, Nd, Sr, Zr, and Y are also enhanced to some degree compared with solar r-process pattern.

5. Conclusion

Using the "snapshot" spectra from HERES survey, we derived the thorium abundances of 77 metal-poor stars, 17 of which have detected Th abundance, while for the rest, only upper limits are available. Thorium abundances cover a wide range of about 4.0 dex, and a scatter exists in the distribution of log(Th/Eu) ratios, supporting previous studies suggesting that the r-process is not universal. For the five common stars, our results are in good agreement with previous studies, which gives us the confidence to present a reliable Th distribution and to discuss r-process pattern for such a large sample of metal-poor stars.

With avaliabe abundances, we explored the correlation between Th and other r-process elements. We confirmed the relatively large scatter in log(Th/Ba) and log(Th/Sr) distributions, and found that a better consistence exists within r-process stars,

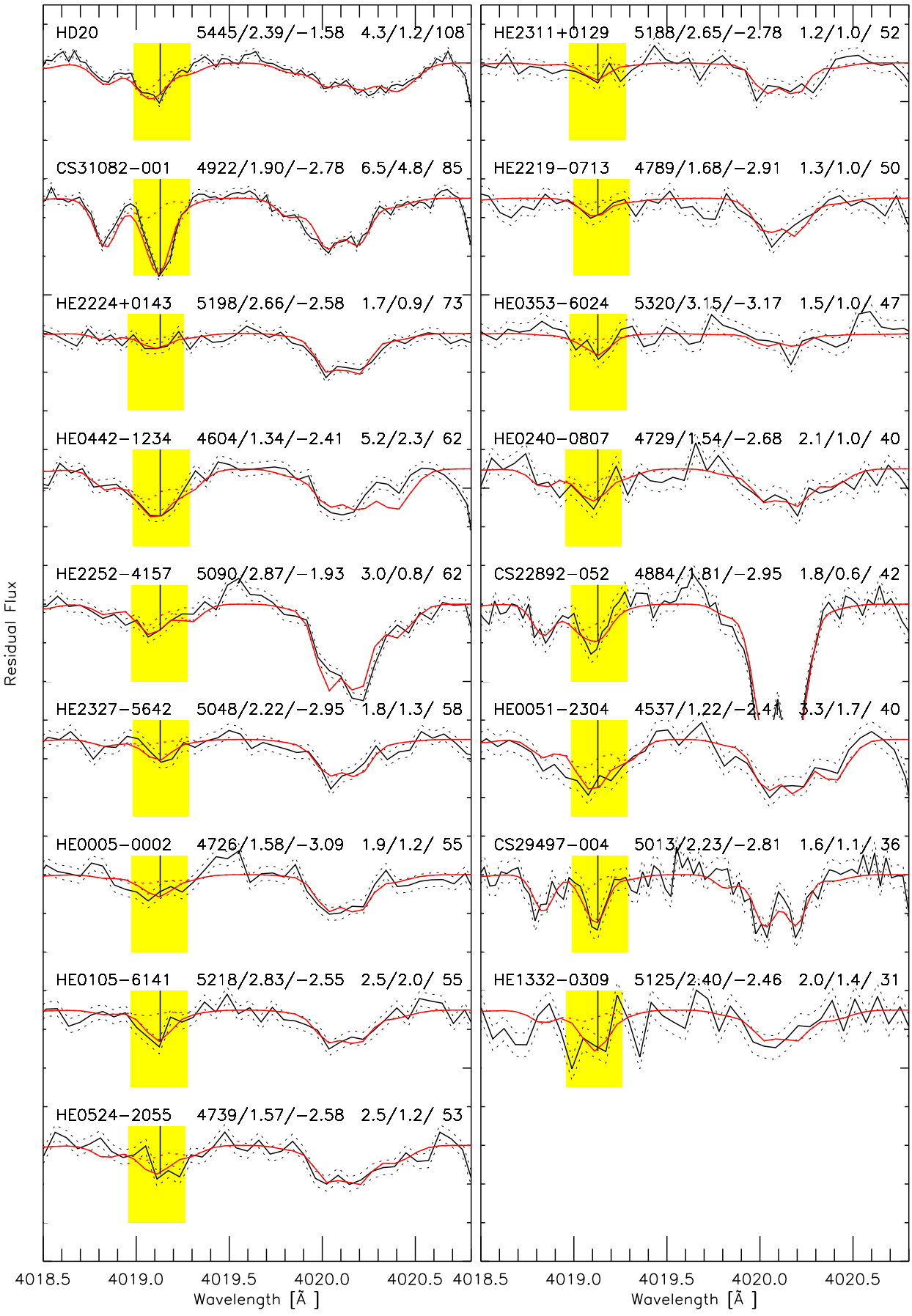

Fig. 7. Th II line profile fits for stars with detected thorium abundances above 1σ. Fitting regions are highlighted in bright yellow. **Black Solid:** observed spectrum; **Black Dotted:** observed spectrum including noise; **Red Solid:** best fit synthetic spectrum; **Red Dotted:** best synthetic spectrum after removing the Th II line.

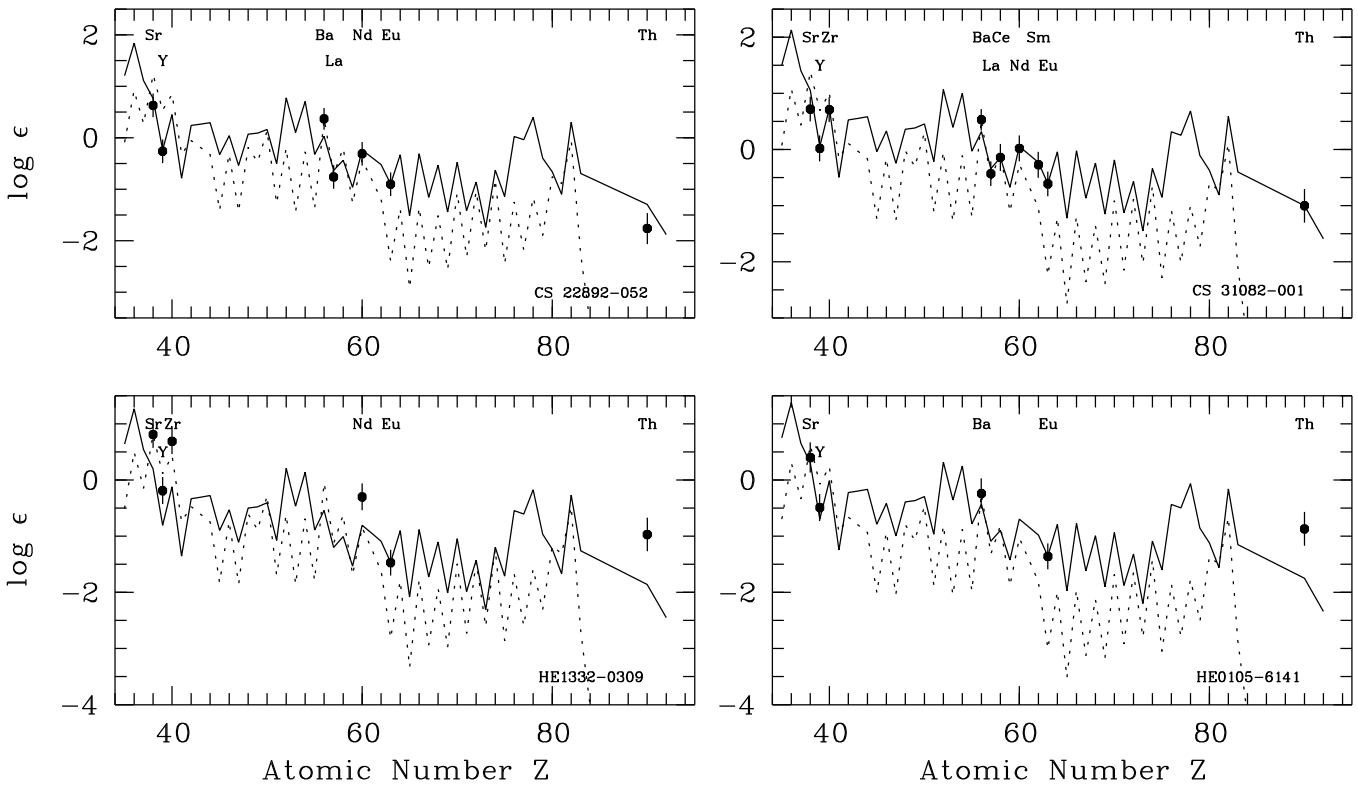

Fig. 8. Abundance pattern of CS 22892−052, CS 31082−001, HE 1332−0309 and HE 0105−6141, compared with the solar r-process pattern (solid line) scaled to the Eu abundance and the solar s-process pattern (dotted line) scaled to the Ba or Sr abundance of each star. The r- and s- fractions are from Arlandini et al. (1999), except for Th and U which are from Burris et al. (2000).

which confirms that these stars formed from the gas experienced similar nucleosynthesis.

Using log(Th/Eu) as the chronometer, we derived the ages for r-process metal-poor stars, for which both Th and Eu are available. Two stars might be "actinide boosted", considering an error to 11.7 Gyr in our age estimation. These stars might have experienced very different chemical enrichments during their formation and evolution. At present the only possible explanation would be that, the r-process elements in these stars were implanted long after the formation of the star, still holding the principle of a universal r-process pattern. It suggests that "actinide boost" might not be a rare phenomenon, thus questioning the reliability in using $\log(\mathrm{Th/X_{stable}})$ for cosmochronometry to derive stellar ages. For this kind of stars, U abundances are needed to confirm the "actinide boost" feature and log(Th/U) can be used to give more accurate age estimations.

However, it should be cautioned again that, 1σ detection significance was adopted in this work, due to the weakness of Th II line and the limited quality of our present data, which may lead to significant uncertainty in the thorium abundance. Thus, the detection of Th in stars without enhancement of other n-capture elements and the "actinide boost" phenomenon in some stars are not confirmed conclusion. Better quality spectra are needed for higher precision Th and other r-process heavy elements abundance determinations. Thus here we would not like to give any conclusion, but rather to draw attention on those very interesting objects from this work, i.e., HE 2219−0713, HE 0305−6024, HE 0105−6141 and HE 1332−0309. Actually we ourselves have already submitted a proposal for the observation time using ESO VLT/UVES for obtaining better quality data of these objects, if some of them can be confirmed, it will be a very important discovery.

Acknowledgements. The authors would like to give thanks to Dr. Paul Barklem for improving and running the code, for modifying and commenting on the paper draft, especially for his contribution to writing Sect. 3, as well as for his enthusiasm on this work. J.R. and N.C. acknowledge financial support by the Research Links program of the Swedish Research Council, the Global Networks program of Universität Heidelberg, and by Deutsche Forschungsgemeinschaft through grant CH 214/5-1 and Sonderforschungsbereich SFB 881 The Milky Way System (subprojects A4 and A5). J.R. and G.Z. acknowledge the support by NSFC grant No. 10821061.

References

Aoki, W., Honda, S., Sadakane, K., & Arimoto, N. 2007, PASJ, 59, L15
Arlandini, C., Käppeler, F., Wisshak, K., et al. 1999, ApJ, 525, 886
Barklem, P. S., Christlieb, N., Beers, T. C., et al. 2005, A&A, 439, 129
Beers, T. C. & Christlieb, N. 2005, ARA&A, 43, 531
Burris, D. L., Pilachowski, C. A., Armandroff, T. E., et al. 2000, ApJ, 544, 302
Cayrel, R., Hill, V., Beers, T. C., et al. 2001, Nature, 409, 691
Christlieb, N., Beers, T. C., Barklem, P. S., et al. 2004, A&A, 428, 1027
Cohen, J. G., Christlieb, N., Qian, Y., & Wasserburg, G. J. 2003, ApJ, 588, 1082
Cowan, J. J., Pfeiffer, B., Kratz, K., et al. 1999, ApJ, 521, 194
Cowan, J. J., Sneden, C., Burles, S., et al. 2002, ApJ, 572, 861

Table 4. Stars with detected Th abundances classified into different subclasses of metal-poor stars.

Name	$T_{\rm eff}$ [K]	log$g$ [cm s^{-2}]	[Fe/H]	logϵ(Th)	[Th/Fe]	log(Th/Eu)	"Age" [Gyr]
			r-I stars				
HD 20	5445	2.39	−1.58	−1.06	0.43	−0.79	23.8
HE 0105−6141	5218	2.83	−2.55	−0.87	1.59	0.49	−38
HE 0240−0807	4729	1.54	−2.68	−1.90	0.69	−0.47	6.5
HE 0442−1234	4604	1.34	−2.41	−1.91	0.41	−0.53	9.3
HE 0524−2055	4739	1.57	−2.58	−1.91	0.58	−0.32	−0.5
HE 2252−4157	5090	2.87	−1.93	−1.32	0.52	−0.43	4.7
			r-II stars				
CS 22892−052	4884	1.81	−2.95	−1.76	1.10	−0.86	24.7
CS 29497−004	5013	2.23	−2.81	−1.17	1.55	−0.49	7.5
CS 31082−001	4922	1.90	−2.78	−1.00	1.69	−0.39	2.8
HE 2224+0143	5198	2.66	−2.58	−1.47	1.02	−0.45	5.6
HE 2327−5642	5048	2.22	−2.95	−1.45	1.41	−0.25	−3.7
			r-normal stars				
HE 0051−2304	4537	1.22	−2.41	−1.94	0.38	−0.19	−6.5
			unclassified stars				
HE 0005−0002	4726	1.58	−3.09	−2.03	0.97	-	-
HE 0353−6024	5320	3.15	−3.17	−1.06	2.02	-	-
HE 1332−0309	5125	2.40	−2.46	−0.97	1.40	0.5	−38.7
HE 2219−0713	4789	1.68	−2.91	−1.97	0.85	-	-
HE 2311+0129	5188	2.65	−2.78	−1.32	1.37	-	-

Frebel, A., Christlieb, N., Norris, J. E., et al. 2007, ApJ, 660, L117
Goriely, S. & Arnould, M. 2001, A&A, 379, 1113
Goriely, S. & Clerbaux, B. 1999, A&A, 346, 798
Hayek, W., Wiesendahl, U., Christlieb, N., et al. 2009, A&A, 504, 511
Hill, V., Plez, B., Cayrel, R., et al. 2002, A&A, 387, 560
Honda, S., Aoki, W., Ishimaru, Y., & Wanajo, S. 2007, ApJ, 666, 1189
Honda, S., Aoki, W., Kajino, T., et al. 2004, ApJ, 607, 474
Ivans, I. I., Simmerer, J., Sneden, C., et al. 2006, ApJ, 645, 613
Johnson, J. A. 2002, ApJS, 139, 219
Johnson, J. A. & Bolte, M. 2001, ApJ, 554, 888
Jonsell, K., Barklem, P. S., Gustafsson, B., et al. 2006, A&A, 451, 651
Kratz, K., Farouqi, K., Pfeiffer, B., et al. 2007, ApJ, 662, 39
Kupka, F., Piskunov, N., Ryabchikova, T., Stempels, H., & Weiss, W. 1999, A&AS, 138, 119
Lucatello, S., Beers, T. C., Christlieb, N., et al. 2006, ApJ, 652, L37
Mashonkina, L., Christlieb, N., Barklem, P. S., et al. 2010, A&A, 516, A46+
McWilliam, A. 1998, AJ, 115, 1640
Nilsson, H., Zhang, Z., Lundberg, H., & Nordström, S. J. B. 2002, A&A, 382, 368
Norris, J. E., Ryan, S. G., & Beers, T. C. 2001, ApJ, 561, 1034
Plez, B., Hill, V., Cayrel, R., et al. 2004, A&A, 428, L9
Roederer, I. U., Kratz, K., Frebel, A., et al. 2009, ApJ, 698, 1963
Schatz, H., Toenjes, R., Pfeiffer, B., et al. 2002, ApJ, 579, 626
Simmerer, J., Sneden, C., Cowan, J. J., et al. 2004, ApJ, 617, 1091
Sneden, C., Cowan, J. J., Ivans, I. I., et al. 2000, ApJ, 533, L139
Sneden, C., Cowan, J. J., Lawler, J. E., et al. 2003, ApJ, 591, 936
Sneden, C., Lawler, J. E., Cowan, J. J., Ivans, I. I., & Den Hartog, E. A. 2009, ApJS, 182, 80
Sneden, C., McWilliam, A., Preston, G. W., et al. 1996, ApJ, 467, 819
Truran, J. W., Cowan, J. J., Pilachowski, C. A., & Sneden, C. 2002, PASP, 114, 1293
Valenti, J. A. & Piskunov, N. 1996, A&AS, 118, 595
Wanajo, S., Itoh, N., Ishimaru, Y., Nozawa, S., & Beers, T. C. 2002, ApJ, 577, 853
Yong, D., Karakas, A. I., Lambert, D. L., Chieffi, A., & Limongi, M. 2008a, ApJ, 689, 1031
Yong, D., Lambert, D. L., Paulson, D. B., & Carney, B. W. 2008b, ApJ, 673, 854
Yushchenko, A., Gopka, V., Goriely, S., et al. 2005, A&A, 430, 255
Zhang, L., Karlsson, T., Christlieb, N., et al. 2010, ArXiv e-prints

Table 5. Summary of abundance results for stars with Th abundances from this work. Except for Th, other element abundances and the stellar parameters are from Paper II. The errors are discussed in the text. m and m' are the detection levels for Th II 4019.129 line profile fit with and without blendings.

Name	$T_{\rm eff}$ [K]	log$g$ [cm s^{-2}]	[Fe/H]	$V_{\rm mic}$ [kms^{-1}]	logϵ(Th)	[Th/Fe]	[Eu/Fe]	[Ba/Eu]	log(Th/Eu)	[C/Fe]	$m(\sigma)$	$m'(\sigma)$
CS 22175−007	5108	2.46	−2.81	1.67	< −1.07	< 1.65	-	-	-	0.19	0.39	0.15
CS 22886−042	4881	1.85	−2.68	1.84	< −1.53	< 1.06	-	-	-	0.01	0.67	0.48
CS 22892−052	4884	1.81	−2.95	1.67	−1.76	1.10	1.54	−0.35	−0.86	1.00	1.81	0.61
CS 22945−028	5126	2.55	−2.66	1.53	< −0.99	< 1.58	-	-	-	0.21	0.49	0.33
CS 29491−069	5103	2.45	−2.81	1.54	< −1.37	< 1.35	1.06	−0.72	< −0.13	0.18	0.45	0.20
CS 29497−004	5013	2.23	−2.81	1.62	−1.17	1.55	1.62	−0.41	−0.49	0.22	1.63	1.12
CS 29510−058	5108	2.32	−2.61	1.62	< −1.20	< 1.32	-	-	-	0.40	0.24	0.08
CS 31082−001	4922	1.90	−2.78	1.88	−1.00	1.69	1.66	−0.48	−0.39	0.22	6.50	4.81
HD 20	5445	2.39	−1.58	2.30	−1.06	0.43	0.80	−0.49	−0.79	−0.34	4.27	1.35
HE 0005−0002	4726	1.58	−3.09	1.82	−2.03	0.97	-	-	-	0.17	1.90	1.19
HE 0023−4825	5816	3.63	−2.06	1.45	< −0.55	< 1.42	-	-	-	0.31	0.61	0.16
HE 0029−1839	5010	2.19	−2.50	1.67	< −2.60	< 0.19	-	-	-	0.31	1.13	0.28
HE 0039−4154	4735	1.55	−3.38	2.01	< −2.39	< 0.9	-	-	-	−0.14	0.84	0.40
HE 0043−2845	5517	4.42	−2.91	1.17	< −0.60	< 2.22	-	-	-	0.19	0.21	0.14
HE 0051−2304	4537	1.22	−2.41	1.97	−1.94	0.38	0.17	−0.24	−0.19	−0.64	3.30	1.71
HE 0054−0657	5908	4.40	−2.00	1.56	< 0.02	< 1.93	-	-	-	0.29	0.43	0.10
HE 0105−6141	5218	2.83	−2.55	1.66	−0.87	1.59	0.68	−0.51	0.49	0.20	2.48	2.10
HE 0109−3711	6156	3.91	−1.91	1.60	< 0.57	< 2.39	-	-	-	0.31	0.28	0.14
HE 0121−2826	4955	1.99	−2.97	1.68	< −1.70	< 1.18	-	-	-	0.54	0.32	0.12
HE 0143−1135	5629	4.53	−2.13	1.42	< −0.38	< 1.66	-	-	-	0.23	0.72	0.25
HE 0240−0807	4729	1.54	−2.68	1.96	−1.90	0.69	0.73	−0.52	−0.47	−0.35	2.10	1.05
HE 0300−0751	5280	2.97	−2.27	1.61	< −1.07	< 1.11	0.77	−0.75	< −0.08	0.10	0.98	0.61
HE 0315+0000	5013	2.11	−2.73	1.72	< −1.76	< 0.88	0.65	−0.31	< −0.19	0.18	1.21	0.75
HE 0323−4529	5127	2.51	−3.15	1.62	< −1.36	< 1.70	-	-	-	0.38	0.90	0.66
HE 0328−1047	5301	3.03	−2.25	1.21	< −1.54	< 0.62	0.42	-0.49	< −0.23	0.15	0.88	0.25
HE 0330−4144	5961	4.20	−1.90	1.52	< −0.23	< 1.58	-	-	-	0.19	0.52	0.16
HE 0340−5355	4862	1.81	−2.89	1.87	< −2.01	< 0.79	-	-	-	−0.11	0.90	0.52
HE 0341−4024	6108	4.20	−1.82	1.41	< −0.48	< 1.25	0.69	−0.77	< 0.14	0.27	1.01	0.43
HE 0347−1819	5198	4.23	−2.78	1.61	< −0.84	< 1.85	-	-	-	0.03	0.34	0.18
HE 0353−6024	5320	3.15	−3.17	1.49	−1.06	2.02	-	-	-	0.29	1.46	1.00
HE 0442−1234	4604	1.34	−2.41	2.21	−1.91	0.41	0.52	−0.65	−0.53	−0.61	5.18	2.16
HE 0450−4705	5429	3.34	−3.10	1.49	< −1.00	< 2.01	-	-	-	0.84	0.53	0.17
HE 0501−5139	5861	3.54	−2.38	1.49	< 0.11	< 2.4	-	-	-	0.40	0.20	0.17
HE 0520−1748	5272	3.06	−2.52	1.46	< −1.82	< 0.61	-	-	-	0.45	1.59	0.92
HE 0524−2055	4739	1.57	−2.58	1.95	−1.91	0.58	0.49	−0.42	−0.32	−0.25	2.48	1.34
HE 0534−4615	5506	3.40	−2.01	1.43	< −1.15	< 0.77	0.49	−0.50	< −0.15	0.13	1.05	0.28
HE 0926−0508	6249	4.24	−2.78	1.60	< −0.40	< 2.29	-	-	-	0.62	0.21	0.12
HE 1052−2548	6534	4.52	−2.29	1.57	< 0.06	< 2.26	-	-	-	0.51	0.73	0.63
HE 1100−0137	6101	4.25	−2.92	1.29	< −0.02	< 2.81	-	-	-	0.47	0.17	0.17
HE 1124−2335	5226	2.68	−2.95	1.65	< −1.41	< 1.45	-	-	-	0.86	0.53	0.11
HE 1126−1735	5689	3.31	−2.69	1.55	< −0.84	< 1.76	-	-	-	0.23	0.68	0.15
HE 1127−1143	5224	2.64	−2.73	1.59	< −1.31	< 1.33	1.08	−0.45	< −0.17	0.54	1.10	0.76
HE 1132+0204	5046	2.25	−2.55	1.68	< −1.65	< 0.81	0.25	−0.94	< 0.12	0.13	1.41	0.95
HE 1207−2031	6281	4.40	−2.82	1.42	< 0.00	< 2.73	-	-	-	0.64	0.94	0.69
HE 1221−1948	6083	3.81	−2.60	1.65	< −0.26	< 3.01	-	-	-	1.42	1.46	1.36
HE 1225+0155	4842	1.80	−2.75	1.85	< −2.50	< 0.16	0.25	−0.70	< −0.51	0.26	0.90	0.23
HE 1245−1616	6191	4.04	−2.98	1.53	< −0.03	< 2.86	-	-	-	0.77	0.79	0.73
HE 1246−1344	4853	1.65	−3.40	1.84	< −2.16	< 1.15	-	-	-	−0.06	0.89	0.30
HE 1247−2114	5012	2.08	−2.61	1.67	< −1.87	< 0.65	0.22	−0.65	< 0.01	0.32	1.26	0.66
HE 1251−0104	5084	2.32	−2.73	1.58	< −1.64	< 1.00	-	-	-	0.25	0.83	0.46
HE 1256−0651	6137	4.05	−2.36	1.50	< −0.23	< 2.04	-	-	-	0.62	0.93	0.45
HE 1300−0642	5173	2.68	−3.03	1.57	< −1.25	< 1.69	-	-	-	0.34	0.49	0.24
HE 1300−2431	5029	1.96	−3.25	1.92	< −1.82	< 1.34	-	-	-	−0.16	0.95	0.47
HE 1305−0331	6081	4.22	−3.26	1.58	< −0.28	< 2.89	-	-	-	1.13	0.78	0.29
HE 1330−0354	6257	4.13	−2.29	1.49	< 0.04	< 2.24	-	-	-	1.05	0.54	0.31
HE 1332−0309	5125	2.40	−2.46	1.64	−0.97	1.40	0.48	−0.48	0.50	0.21	1.96	1.43
HE 1337−0453	5938	3.56	−2.34	1.62	< −0.41	< 1.84	-	-	-	0.12	0.46	0.23

Table 5. Continued.

Name	$T_{\rm eff}$ [K]	log$g$ [cm s^{-2}]	[Fe/H]	$V_{\rm mic}$ [kms^{-1}]	logϵ(Th)	[Th/Fe]	[Eu/Fe]	[Ba/Eu]	log(Th/Eu)	[C/Fe]	m(σ)	m'(σ)
HE 1431−2142	6137	4.10	−2.60	1.55	< -0.20	< 2.31	-	-	-	0.48	0.60	0.23
HE 2133−1432	5716	3.46	−2.02	1.46	< -0.82	< 1.11	-	-	-	0.12	1.10	0.60
HE 2134+0001	5257	3.00	−2.22	1.55	< -1.36	< 0.77	0.47	−0.89	< -0.12	0.20	1.17	0.52
HE 2151−2858	5598	4.14	−2.38	1.39	< -0.43	< 1.86	-	-	-	0.10	0.68	0.51
HE 2153−2719	4898	2.01	−2.49	1.80	< -2.81	< -0.41	0.21	−0.90	< -1.04	0.12	0.95	0.24
HE 2158−3112	4843	1.85	−2.75	1.85	< -2.81	< -0.15	0.02	−0.86	< 0.60	−0.04	1.31	0.42
HE 2219−0713	4789	1.68	−2.91	1.64	−1.97	0.85	-	-	-	−0.17	1.35	0.97
HE 2224+0143	5198	2.66	−2.58	1.67	−1.47	1.02	1.05	−0.46	−0.45	0.35	1.72	0.99
HE 2224−4103	5074	2.32	−2.64	1.75	< -1.71	< 0.84	-	-	-	0.23	0.90	0.45
HE 2229−4153	5138	2.47	−2.62	1.79	< -1.91	< 0.62	0.45	−0.73	< -0.28	0.37	0.79	0.20
HE 2234−0521	5332	3.15	−2.78	1.39	< -0.93	< 1.76	-	-	-	0.36	0.27	0.07
HE 2247−3705	5366	3.04	−2.27	1.48	< -1.39	< 0.79	-	-	-	0.36	0.76	0.27
HE 2250−2132	5705	3.69	−2.22	1.43	< -0.74	< 1.39	-	-	-	0.41	0.89	0.43
HE 2252−4157	5090	2.87	−1.93	1.55	−1.32	0.52	0.53	−0.24	−0.43	−0.15	2.98	1.34
HE 2259−3407	6266	4.32	−2.29	1.37	< 0.00	< 2.2	-	-	-	0.41	0.39	0.16
HE 2311+0129	5188	2.65	−2.78	1.54	−1.32	1.37	-	-	-	0.33	1.24	1.05
HE 2326+0038	5145	2.51	−2.77	1.62	< -1.59	< 1.09	-	-	-	0.23	0.51	0.11
HE 2327−5642	5048	2.22	−2.95	1.69	−1.45	1.41	1.22	−0.56	−0.25	0.43	1.79	1.35
HE 2338−1618	5515	3.38	−2.65	1.43	< -0.76	< 1.80	-	-	-	0.47	0.88	0.56
HE 2345−1919	5617	4.46	−2.46	1.47	< -0.47	1.90	-	-	-	0.24	0.97	0.60

Table 6. Thorium and europium abundances from previous works (From the summary of SAGA database and Roederer et al. 2009). Both detected values and upper limits are included.

name	[Fe/H]	logϵ(Th)	logϵ(Eu)	log(Th/Eu)	"Age" [Gyr]	Ref.
BD+08_2856	-2.10	-1.78 ± 0.10	-1.16 ± 0.06	-0.62	13.5	1,2
BD+17_3248	-2.23	-1.18 ± 0.10	-0.67 ± 0.05	-0.51	8.4	3
BD+04_2621	-2.50	< -3.12	-2.61 ± 0.23	< -0.51	> 8.4	1,2
BD$-$18_5550	-3.03	< -3.10	-2.79 ± 0.22	< -0.31	> -0.9	1,2
CS22892$-$052	-2.92	-1.42 ± 0.15	-0.86 ± 0.02	-0.56	10.7	7
CS29491$-$069	-2.60	-1.43 ± 0.22	-1.03 ± 0.10	-0.40	3.3	3
CS29497$-$004	-2.81	-0.96 ± 0.15	-0.45 ± 0.20	-0.28	-2.3	4,5
CS30306$-$132	-2.40	-1.12 ± 0.15	-1.14 ± 0.25	0.02	-16.3	7
CS31078$-$018	-2.84	-1.35 ± 0.25	-1.17 ± 0.17	-0.18	-7.0	8
CS31082$-$001	-2.90	-0.98 ± 0.05	-0.76 ± 0.11	-0.22	-5.1	8,9,10
HD108317	-2.18	-1.84 ± 0.20	-1.32 ± 0.05	-0.52	8.9	3
HD108577	-2.36	-2.11 ± 0.14	-1.48 ± 0.02	-0.63	14.0	1,2
HD110184	-2.52	-2.50 ± 0.15	-1.91 ± 0.05	-0.59	12.1	7
HD115444	-2.85	-1.97 ± 0.15	-1.64 ± 0.03	-0.33	0.0	3
HD122563	-2.72	< -2.43	-2.75 ± 0.11	< 0.32	> -30.3	3
HD122956	-1.95	-1.50 ± 0.17	-0.94 ± 0.07	-0.56	10.7	3
HD126587	-2.93	< -2.39	-1.97 ± 0.06	< -0.42	> 4.2	3
HD128279	-2.00	< -2.00	-1.57 ± 0.06	< -0.43	> 4.7	2,18
HD175305	-1.48	-0.76 ± 0.15	-0.36 ± 0.07	-0.40	3.3	3
HD186478	-2.50	-1.85 ± 0.15	-1.34 ± 0.06	-0.51	8.4	7
HD204543	-1.87	-1.68 ± 0.14	-1.05 ± 0.07	-0.63	14.0	6
HD221170	-2.20	-1.46 ± 0.05	-0.86 ± 0.07	-0.60	12.6	11
HD6268	-2.40	-1.93 ± 0.10	-1.56 ± 0.03	-0.37	1.9	3
HD74462	-1.52	-0.94 ± 0.13	-0.50 ± 0.09	-0.44	5.1	3
HD88609	-3.07	< -2.65	-2.89 ± 0.12	< 0.24	> -27	19
HE0338$-$3945	-2.42	< 0.23	0.02 ± 0.17	< 0.21	> -25	6
HE1219$-$0312	-2.97	-1.29 ± 0.14	-1.06 ± 0.10	-0.23	-4.7	3
HE1523$-$0901	-2.95	-1.20 ± 0.05	-0.62 ± 0.05	-0.58	11.7	12
HE2148$-$1247	-2.50	< -0.50	0.17 ± 0.10	< -0.67	> 15.9	20
HE2327$-$5642	-2.78	-1.67 ± 0.21	-1.29 ± 0.07	-0.38	2.3	13
M15 K341	-2.32	-1.51 ± 0.10	-0.88 ± 0.09	-0.63	14.0	14
M15 K462	-2.25	-1.30 ± 0.10	-0.61 ± 0.09	-0.69	16.8	14
M15 K583	-2.34	-1.70 ± 0.10	-1.24 ± 0.09	-0.46	6.1	14
M5 IV$-$81	-1.28	-0.58 ± 0.15	-0.31 ± 0.05	-0.27	-2.8	15,16
M5 IV$-$82	-1.33	-0.68 ± 0.15	-0.23 ± 0.05	-0.45	5.6	15,16
M92 VII$-$18	-2.29	-2.01 ± 0.07	-1.45 ± 0.07	-0.56	10.7	1,2
UMi COS82	-1.42	-0.25 ± 0.15	0.34 ± 0.11	-0.59	12.1	17

References. (1) Johnson (2002); (2) Johnson & Bolte (2001); (3) Roederer et al. (2009); (4) Christlieb et al. (2004); (5) Barklem et al. (2005); (6) Jonsell et al. (2006); (7) Honda et al. (2004); (8) Hill et al. (2002); (9) Plez et al. (2004); (10) Sneden et al. (2009); (11) Ivans et al. (2006); (12) Frebel et al. (2007); (13) Mashonkina et al. (2010); (14) Sneden et al. (2000); (15) Yong et al. (2008a); (16) Yong et al. (2008b); (17) Aoki et al. (2007); (18) Simmerer et al. (2004); (19) Honda et al. (2007); (20) Cohen et al. (2003).